

NUMERICAL MODEL FOR ANALYSIS OF A FINNED SPACE RADIATOR IN CRITICAL CASES OF OPERATION

Rafael Dias Vilela

Ezio Castejon Garcia

Instituto Tecnológico de Aeronáutica (ITA) - Departamento de Engenharia Aeronáutica e Mecânica, Área de Aerodinâmica Propulsão e Energia - Pr. Marechal Eduardo Gomes, 50 - Vila das Acácias CEP 12228-900 – São José dos Campos – SP – Brasil
 rdiasvilela@yahoo.com.br
 ezio@ita.br

Abstract. Artificial satellites are subject, from time to time, a wide temperature variation due to their orbits. On the other hand, the equipment that make up feature limits (minimum and maximum) of temperature must not be exceeded so that the satellite's operation is not compromised. In this way, this work presents a numerical analysis of a spatial finned radiator connected to a satellite in critical conditions of operation. Such a device is designed to operate in passive thermal control of satellites keeping temperatures within the pre-established limits. From a two-dimensional approach, the resulting equations conductive-radioactive coupling were discretized by finite volume method and solved by the TDMA method (Tri-Diagonal Matrix Algorithm) combined with an iterative process. With the results obtained in FORTRAN code, it was possible to get the temperature profile in the base-fin and hold the balance of energy by radiation. In addition to that, these results can be used in the preparation of projects for thermal control of spacecraft.

Keywords: Finned Radiator, Numeric Model, Critical Cases, Finite Volume Method, Two Dimensional

1. INTRODUCTION

Artificial satellites are subject to large temperature gradients due to the conditions of its operation. In addition to receiving the radiation coming from the Sun and the Earth's albedo, have electric and electronic components that generate heat causing an increase in temperature. On the other hand, when the satellite passes by eclipse, the absence of solar radiation causes a sharp decline in temperatures. Given this, a space radiator can be used so that the temperature variation in the satellite does not exceed the thermal limits specified by the manufacturers of the equipment.

We can consider the Sun as a black body with a temperature of approximately 6000 K issuing 98% of its radiation in a strip of waves between 0 and 3 μm (solar band). In turn, the space radiator, operating at temperatures below 400 K, emits 99.8% of their radiation waves whose length is greater than 3 μm (infrared band-I.V). Soon, the space radiator, predominantly, absorbs radiation in the solar band and issues in the infrared band (Saboya .1987). So, a space radiator receives an optical treatment in order to lower your band solar absorptivity and increase its emissivity in the infrared band.

It is possible to find in the literature studies about space radiators of different types. Cuco *et al.* (2008) have developed a finned radiator with emissivity variable to reduce the need for electric heaters. According to this study, the increase in radiator mass compensates for the energy saving electric that would be taken up with the heaters. This energy saving is of great importance to projects of this kind, because such a feature is usually limited. Lieblein and Diedrich (1975) conducted a study on materials and geometries used in the construction of space radiators on the basis of size, mass, the simplicity of manufacture and heat transfer rate that the device provides. This study also shows that the requirements outlined above are usually in conflict. Garcia (1996) presented a one-dimensional numerical model that analyzes the conductive-radioactive coupling in a radiator with rectangular fins shown in Fig. 1. The study shows the good performance of the radiator, the temperature profile in the base set-flip, the radiosidades (solar and I.V) and heat loss by radiation (solar and I.V). Kumar et al. (1993) propose a space radiator optimization with rectangular fins on the basis of the number of fins and the consequent increase of the weight of the radiator. Present the results obtained in terms of lost heat rate for various numbers of flaps built with three types of different materials (aluminum, steel and brass).

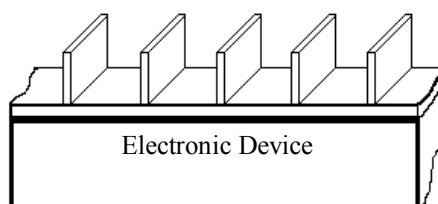


Figure 1. Radiator finned space proposed by Garcia (1996).

The present work aims to study the behavior of the space radiator where critics of the satellite, called operation if hot and cold case. The analysis of the hot case considers the lowest period when it is exposed to the eclipse and the consequent increased incidence of solar radiation and the Earth's albedo. In cold case the satellite remains a longer period under the eclipse thus causing a decrease in incidence solar and Earth's albedo, (Silva, 2009). Therefore, an algorithm has been developed in FORTRAN analysis conductive-radioactive coupling present in radiator. Using a two-dimensional approach, the resulting equations that were discretizadas by coupling finite volume method and resolved with the Tri-Diagonal Matrix Algorithm (TDMA) combined with an iterative process to calculate the temperature profile in the base-plate of the radiator. From the results, the work shows the need (or not) the use of heat pipes and electric heaters for hot and cold-case case respectively.

2. METHODOLOGY

Considering the space radiator shown in Fig. 2 with flat rectangular fins spaced equally and with the same length and thickness is possible treat the problem using the symmetry between the cavities of the radiator.

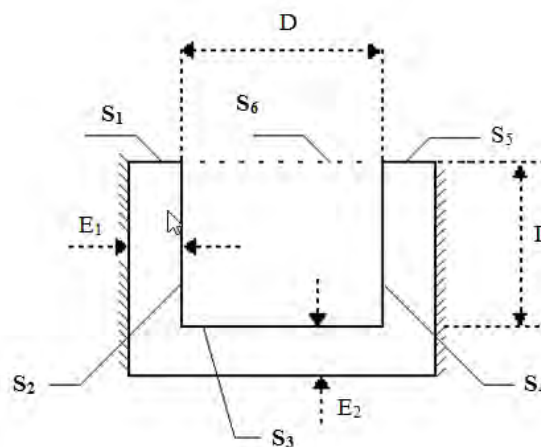


Figure 2. Front view of geometric domain set to the mathematical formulation.

Figure 3 shows that, when we study for a hollow specifies, another axis of symmetry can be used for temperature profile in the base set-flip, because the radiosidades who leave the area S_4 and S_2 and focus also on the surface S_3 . In addition, as can be seen in Fig. 3, the radiosities exchanged between S_2 and S_4 surfaces is the same. The radiosities that let S_2 , S_3 and S_4 surfaces, in which go to space, were obtained by adding of an abstract surface S_6 .

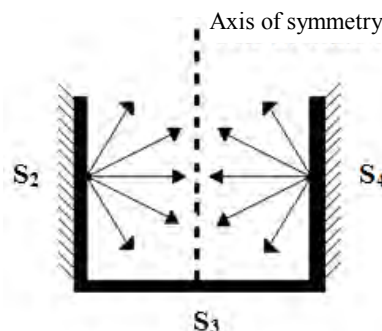


Figure 3. The radiosities that leave S_2 and S_4 are equal and reach S_3 the same way.

The present study takes into account also the following assumptions:

- (1) Solar radiation focusing at right angles with respect to the base of the radiator.
- (2) The Thermo-optical properties of surfaces are constant and independent of temperatures.
- (3) Heat transfer by conduction two-dimensional.
- (4) Steady state without heat generation.
- (5) Isotropic Material.
- (6) Unit depth.

- (7) Adoption of the model of two bands (solar and infrared).
- (8) Emissivity and reflectivity values constant for the two bands.
- (9) Plate surfaces and opaque flip ($\rho = 1 - \epsilon$).
- (10) $\alpha = \epsilon$ for each band (solar and I.V).
- (11) The issue of diffuse surfaces.
- (12) Satellite surface temperature (in contact with the radiator).

3. MATHEMATICAL FORMULATION

The excess heat generated by the components of the satellite is transferred to the predominantly radiator by driving and dissipated into space in the form of radiation. Healthy-differential equations arising from the conductive-radioactive coupling were obtained by performing a power balance in each point of the domain. For the points adjacent to the surfaces S_1 , S_2 and S_3 was adopted the radioactive heat flux boundary condition. Figure 4 shows the distribution, nodal boundary conditions and parameters.

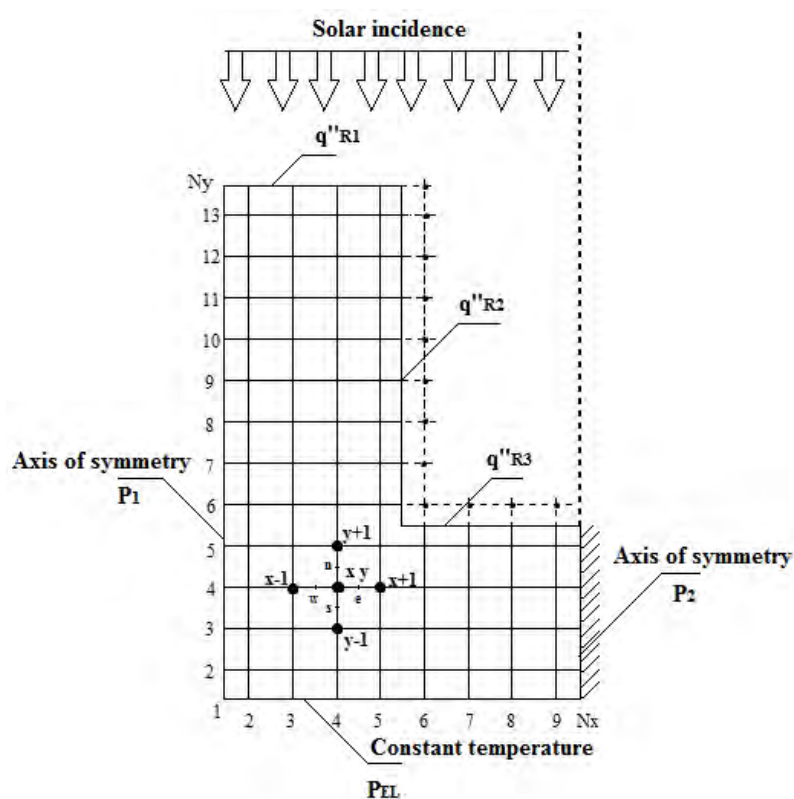


Figure 4. Division of the field by finite volume method.

Fourier's law (2D):

$$\frac{\partial}{\partial x} \left(\frac{\partial T}{\partial x} \right) + \frac{\partial}{\partial y} \left(\frac{\partial T}{\partial y} \right) = 0 \quad (1)$$

“Equation (1)” has been discretized by finite volume method.

$$\left[k.A. \left(\frac{T(x+1, y) - T(x, y)}{\partial x} \right) - k.A. \left(\frac{T(x, y) - T(x-1, y)}{\partial x} \right) \right] + \left[k.A. \left(\frac{T(x, y+1) - T(x, y)}{\partial y} \right) - k.A. \left(\frac{T(x, y) - T(x, y-1)}{\partial y} \right) \right] = 0 \quad (2)$$

Where:

k : thermal conductivity;

A : cross-sectional area;

T : nodal temperature.

From the assumptions adopted, obtaining the equations related to heat transfer by radiation is carried out in a manner similar to that developed by Garcia (1996), including:

Radiosities on solar and infrared bands:

$$B_{Si} = (1 - \varepsilon_{Si}) \cdot \sum_{j=1}^n \int B_{Sj} \cdot dF_{dAi-dAj} \quad (3)$$

$$B_{li} = \varepsilon_{li} \cdot \sigma \cdot T^4(x, y) + (1 - \varepsilon_{li}) \cdot \sum_{j=1}^n \int B_{lj} \cdot dF_{dAi-dAj} \quad (4)$$

Where:

ε_{Si} : absorptivity (solar band) ;

ε_{li} : emissivity (infrared band);

B_{Si} : radiosity (solar band) [W/m²];

B_{li} : radiosity (infrared band) [W/m²];

σ : Stefan-Boltzmann constant [W/m².K⁴].

$dF_{dAi-dAj}$ is the view factor that represents the amount of radiation that leaves the infinitesimal surface i and reaches the infinitesimal surface j . The view factors were obtained in the work of Siegel and Howell, (1972) and Sparrow and Cess, (1978).

Heat flux by radiation on surface S_1 :

$$q_{R1}'' = \varepsilon_{l1} \cdot E_1 \cdot T^4(x, y) - \varepsilon_{S1} \cdot H_{Sol} \cdot E_1$$

Where:

E_i : thickness fin [m];

H_{Sol} : incident solar radiation [W/m²].

(5)

Heat flux by radiation on surfaces S_2 and S_3 :

$$q_{Ri}'' = \frac{\varepsilon_{li} \cdot [\sigma \cdot T_i^4(x, y) - B_{li}(x, y)]}{1 - \varepsilon_{li}} - \frac{\varepsilon_{Si} \cdot B_{Si}(x, y)}{1 - \varepsilon_{Si}} \quad (6)$$

The above equation represents the difference between the radiation emitted in the infrared band and the absorbed radiation in the solar band for each surface of the radiator.

Linearization of the term T_i^4 :

Nonlinearities that occur in the equations were solved with the Taylor series, as described by Shih, (1984).

$$T^4(x, y) = 4 \cdot T'^3(x, y) \cdot T(x, y) - 3 \cdot T'^4(x, y) \quad (7)$$

Where $T'(x, y)$ represents an initial estimate for temperature.

Boundary conditions:

According to Fig. 3 and Fig. 4, we have:

1) For points on S_1 :

$$k \cdot \left(\frac{T(x, y+1) - T(x, y)}{\partial y} \right) = \varepsilon_{fi} \cdot \sigma \cdot [4.T_i'^3(x, y) \cdot T_i(x, y) - 3.T_i'^4(x, y)] - \varepsilon_{Si} \cdot H_{sol} \quad (8)$$

2) For points on S_2 :

$$k \cdot \left(\frac{T(x, y+1) - T(x, y)}{\partial y} \right) = \quad (9)$$

$$= \frac{\varepsilon_{fi}}{(1 - \varepsilon_{fi})} \cdot [\sigma \cdot (4.T_i'^3(x, y) \cdot T_i(x, y) - 3.T_i'^4(x, y)) - B_{fi}(x, y)] - \frac{\varepsilon_{Si} \cdot B_{Si}(x, y)}{1 - \varepsilon_{Si}}$$

3) For points on S_3 :

$$k \cdot \left(\frac{T(x+1, y) - T(x, y)}{\partial y} \right) = \quad (10)$$

$$= \frac{\varepsilon_{fi}}{(1 - \varepsilon_{fi})} \cdot [\sigma \cdot (4.T_i'^3(x, y) \cdot T_i(x, y) - 3.T_i'^4(x, y)) - B_{fi}(x, y)] - \frac{\varepsilon_{Si} \cdot B_{Si}(x, y)}{1 - \varepsilon_{Si}}$$

4) For points on P_1 :

$$k \cdot \left(\frac{T(x, y) - T(x-1, y)}{\partial x / 2} \right) = 0 \quad (11)$$

5) For points on P_2 :

$$k \cdot \left(\frac{T(x+1, y) - T(x, y)}{\partial x / 2} \right) = 0 \quad (12)$$

6) For points on P_{EL} :

$$T(x, y) = T_{EL} \quad (13)$$

Where, T_{EL} represents the temperature of the electronic device.

Dimensionless Characteristic Distance:

In order to show the results, graphically, the following dimensionless parameters were used:

$$X = \frac{x}{D} \quad (14)$$

$$Y = \frac{y}{L} \quad (15)$$

Where x and y represent the nodal distances on the plate and on the fin respectively.

4. NUMERICAL SOLUTION

Once realized the energy balance, equations resulting conductive-radioactive coupling were discretized by finite volume method. First of all, the program calculates the solar band radiosidades for being independent of surface temperatures. On the other hand, the radiosidades in infrared band depends on the surface temperature and, for this reason, it was necessary to arbitrate an initial temperature for such surfaces. Knowing the radiosidades in two bands it was possible to solve the system of equations generated and this way get the temperature profile in the base-plate by two-dimensional TDMA method described by Versteeg and Malalasekera, (1995). Because it is a direct method of solution of systems of equations, the TDMA used in this work had to be combined with an iterative process. At the end of the first iteration the new temperatures obtained override the initial temperatures refereed and the process repeats until the difference between the temperatures of two consecutive iterations is less than the specified tolerance.

After the convergence of the temperatures, the program calculates the flow of heat by radiation in three surfaces analyzed and integrates such streams to get the rates of heat by radiation. The integrals were resolved numerically by the 1/3 Simpson's rule. In addition to that procedure, the calculation of radiosity that leaves the surfaces of the radiator and get lost in space. This was necessary to carry out the radiation energy balance proposed by Garcia, (1996). Figure 5 shows the flowchart of the computational model.

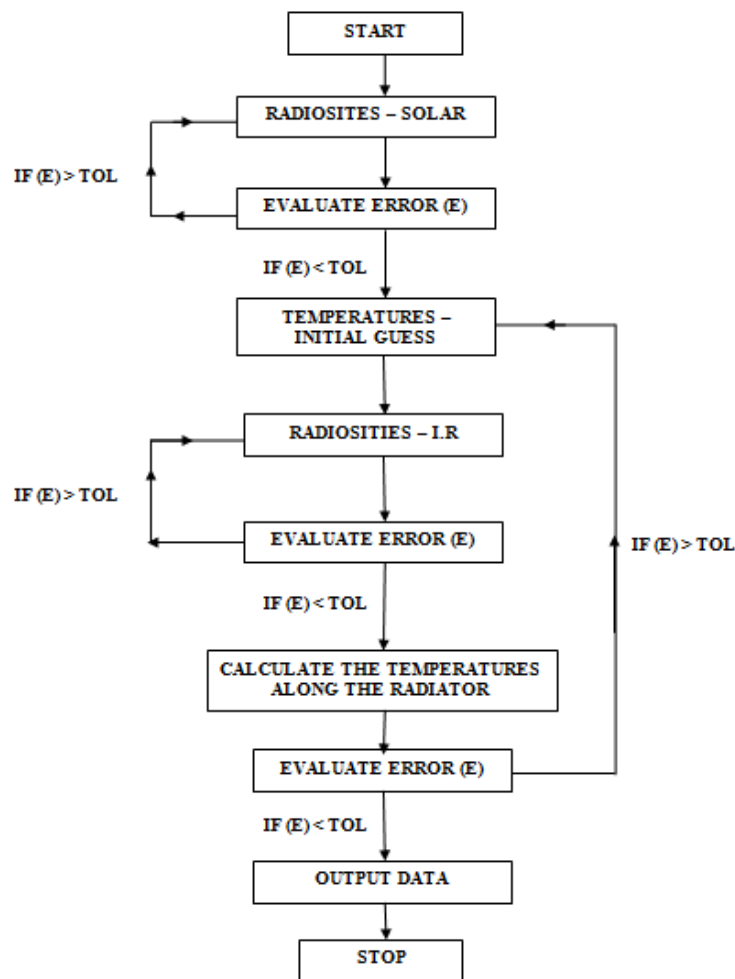


Figure 5. Flowchart of the computational model

5. RESULTS:

The computational model developed allows obtaining the temperature profile in the radiator as a whole. However, the following are only the external surfaces temperature profiles by the fact that the radiation emitted by the radiator depends only on such temperatures. The parameters of the radiator in the study were obtained from the study of Garcia (1996) and are shown in table 1, while Tab. 2 shows the extreme conditions of temperature and solar incidence of hot and cold cases.

Table 1. Dimensions, material properties and tolerances used in numerical simulation.

22nd International Congress of Mechanical Engineering (COBEM 2013)
November 3-7, 2013, Ribeirão Preto, SP, Brazil

N ^o of points	600
L (m)	0,01
D (m)	0,01
E ₁ (m)	0,005
E ₂ (m)	0,005
k (W/m.K)	200
ϵ_{S1}	0,2
ϵ_{S2}	0,2
ϵ_{I1}	0,8
ϵ_{I2}	0,8
Tolerance	10 ⁻⁸

Table 2. Conditions of temperature and solar incidence for both cases.

Critical cases	Hot case	Cold case
T _{EL} (K)	318	263
H _{Sol} (W/m ²)	1400	0

Figure 6 shows the dimensionless temperature profile on the surfaces S₁, S₂ and S₃ to the hot case. We note that the gradients of temperature occurred on the surface S₂ demonstrating good performance of fin. Low gradients were caused by the use of a high thermal conductivity and the small size of the radiator.

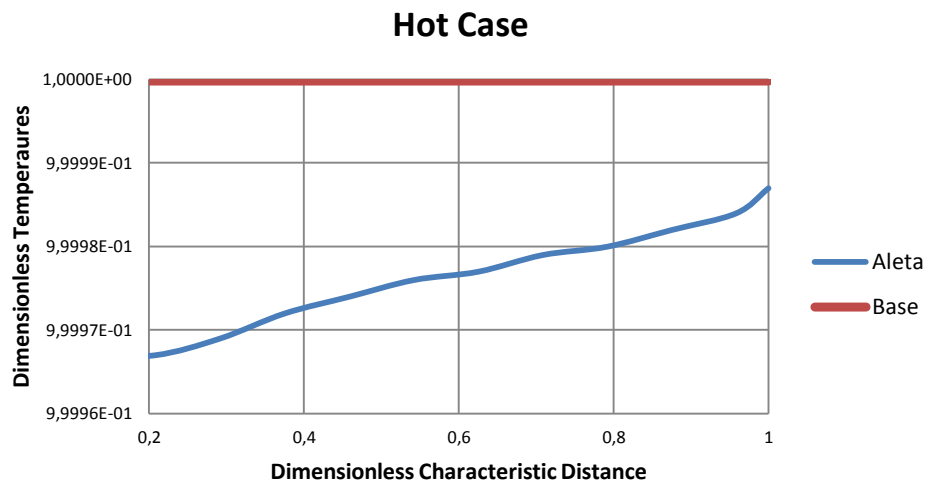


Figure 6. Temperature profile in the base-fin set to the case hot fin.

Figure 7 shows the temperature profile on the surfaces S₁, S₂ and S₃ to the cold-case. The results show the same behavior of obtained for the hot case once again demonstrating the effectiveness of the flap.

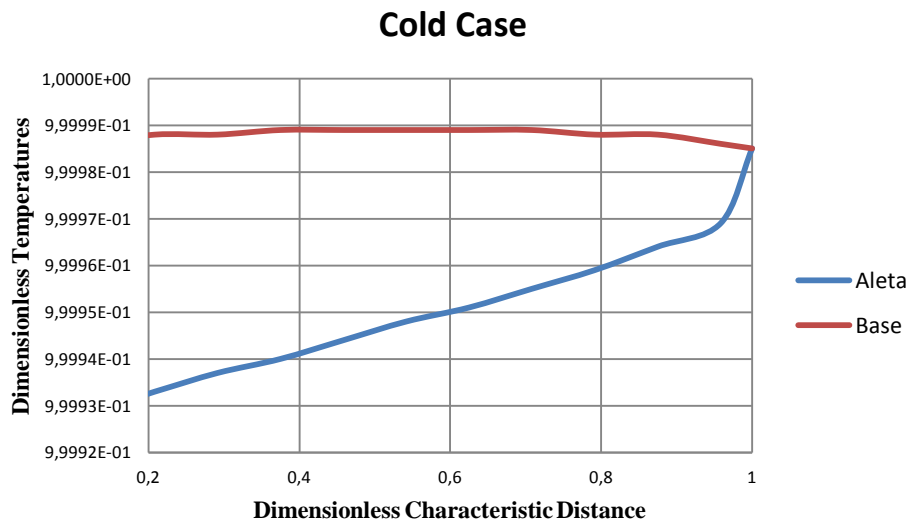


Figure 7. Temperature profile in the base-fin set to the cold case.

6. CONCLUSIONS

This work was performed a numerical simulation of a finned space radiator on a surface of a satellite in order to evaluate the behavior of the set temperatures under critical operation. The use of axis of symmetry shown in Fig. 3 provided the results with a low error and a savings in processing time. The two-dimensional approach did not provide very different results from those found with a one-dimensional approach. This is the thickness of the base and adopted fin. The results showed that the adopted configuration allows a sharper heat exchange between the radiator and the space. This caused the temperatures attained if hot do not exceed the limit specified in advance. Cold case analysis shows that even with the absence of solar radiation the radiator does not compromise the operation of the satellite due to high thermal conductivity. In this case, it becomes unnecessary to use heat pipes to the hot case or heaters for the cold case. This fact, coupled with the low cost of production and the economy of the area provided by the finned radiator demonstrate the advantages of using such a device in the thermal control of satellites.

The next step of this work will be to demonstrate how much the heat rejection will be increased for a given configuration of finned radiator compared to a plane. For future works, the model will be employed to optimize radiators based on the quantity of fins and their dimensions. In addition, it is necessary to analyze the device in conditions where the solar radiation impinges also on the fin surfaces.

7. ACKNOWLEDGMENTS

The authors would like to acknowledge the ITA by the theoretical support and the GSET (Group of Simulation of Flow and Heat Transfer) by the computational support.

8. REFERENCES

- Cuco, A.P.C., Sousa, F.L., Vlassov, V.V. and Neto, A.J.S., 2008. Multi-Objective Design Optimization of a New Space Radiator. *Optimization and Engineering*, Vol 12, pp 393-406.
- Garcia, E.C., 1996. *Condução, Convecção e Radiação Acopladas em Coletores e Radiadores Solares*. Tese de Doutorado, Instituto Tecnológico de Aeronáutica, São José dos Campos.
- Lieblein, S. and Diedrich, J.H., 1965. Material and Geometry Aspects of Space Radiators. *Winter Meeting of the American Society*, Washington, D.C.
- Kumar, S.S.K., Nayak, V. and Venkateshan, S.P., 1993. Optimum finned space radiators. *Int. J. Heat and Fluid Flow*, Vol. 14, No. 2, pp 191-200.
- Saboya, S.M., 1987 “*Análise Térmica de Coletor Solar com Absorvedor Aletado*”, Tese de Doutorado, ITA, São José dos Campos.
- Shih, T.M., 1984. *Numerical Heat Transfer*, Hemisphere, Washington.
- Siegel, R., Howell, J.R., 1972. *Thermal Radiation Heat Transfer*, McGraw-Hill, New York.
- Silva, D.F., 2009. “*Análise de Projeto Preliminar de Controle Térmico do Satélite ITASAT*”, Tese de Mestrado, ITA, São José dos Campos.

22nd International Congress of Mechanical Engineering (COBEM 2013)
November 3-7, 2013, Ribeirão Preto, SP, Brazil

Versteeg, H.K. and Malalasekera, W., 1995. *An Introduction to Computational Fluid Dynamics: The Finite Volume Method*. Longman Scientific & Technical. Harlow Essex, 1st edition.

9. RESPONSIBILITY NOTICE

The author(s) is (are) the only responsible for the printed material included in this paper.